Radiology

# US of the Pediatric Female Pelvis[1]

Harriet J. Paltiel, MD
Andrew Phelps, MD[2]

This review presents the normal and pathologic development of the gonads and genitourinary tract and addresses the role of ultrasonography in the diagnosis and management of gynecologic disorders of the pediatric pelvis, including ambiguous genitalia, prepubertal bleeding, primary amenorrhea, pelvic mass, and pelvic pain.



*Online supplemental material is available for this article.*

[1] From the Department of Radiology, Boston Children's Hospital and Harvard Medical School, 300 Longwood Ave, Boston, MA 02446. Received August 15, 2012; revision requested September 10; revision received April 1, 2013; accepted April 15; final version accepted June 6. **Address correspondence to** H.J.P. (e-mail: *harriet.paltiel@childrens.harvard.edu*).

[2]**Current address:** Department of Radiology and Biomedical Imaging, Benioff Children's Hospital, University of California, San Francisco.

The most common indications for imaging of the pelvis in girls include ambiguous genitalia, prepubertal bleeding, primary amenorrhea, pelvic mass, and pelvic pain. Ultrasonography (US) is the main imaging modality used in the investigation of these disorders with cross-sectional modalities; computed tomography (CT) and magnetic resonance (MR) imaging are generally reserved for further characterization of congenital malformations or tumors (1–4).

## Essentials

- Anomalies of the reproductive tract may manifest at different stages of life; most abnormalities of the external genitalia are obvious at birth, whereas obstructive and nonobstructive lesions of the reproductive tract may be apparent at birth or only later: during childhood, at puberty, in adolescence, or in adulthood.
- In patients with ambiguous genitalia, US is used to determine the location of the gonads and the presence of a uterus.
- US is used to assess ovarian size and morphology and to confirm or exclude a postpubertal appearance of the internal genitalia; US can be used to diagnose an estrogen-secreting adrenal or ovarian tumor and to monitor the effects of medical or surgical treatment.
- Ovarian tumors in the pediatric population are usually benign, with cystic teratoma accounting for more than 90% of all benign ovarian tumors; most cystic teratomas range from 5 to 10 cm in diameter, have a complex appearance, and generally contain fewer than 50% soft-tissue elements by volume.
- In the setting of adnexal torsion, the affected ovary is always enlarged, with a median volume 12 times that of the contralateral normal ovary.
- US is a critical tool in the evaluation of pelvic pain in girls, including those suspected of having acute appendicitis.

## Technique

The pediatric uterus, vagina, and ovaries are optimally imaged when the patient has a full bladder. All patients are therefore asked not to void in the hour prior to undergoing imaging and are encouraged to drink fluids; teenagers are asked to drink 16 ounces.

Transabdominal and linear-array US transducers are generally adequate for most pelvic US examinations. A transperineal approach is useful in young girls with urogenital malformation, hydrometrocolpos, labial mass, or anal atresia (5) (Fig 1). In sexually active adolescents, a transvaginal approach is used to complement the transabdominal examination. In the setting of a complex congenital anomaly, genitography performed with water-soluble contrast material in conjunction with US is often helpful in identification and characterization of the vagina, urogenital sinus, or cloaca.

## Normal Anatomy

The size and shape of the uterus and ovaries are age dependent and subject to hormonal influence. Maternal and placental hormones result in a relatively large size of the neonatal uterus (Fig 2) and ovaries, compared with their size later in infancy, where they remain relatively stable until the first growth spurt occurs at 7 to 8 years of age (6). Mature follicles may be documented within the ovary at all ages, owing to the secretion of follicle-stimulating hormone (7,8) (Fig 3). The prepubertal cervix is equal to or greater in thickness than the uterine fundus, and the endometrial lining is relatively inconspicuous (Fig 4). Uterine length varies, on average, from 2.5 to 4 cm, with a thickness less than or equal to 1 cm. Prepubertal ovarian volume is slightly less than 1 $cm^3$. During puberty, the uterine fundus elongates and thickens and is larger than the cervix; the endometrial lining undergoes cyclical changes associated with the menstrual cycle (9).

## Normal Development of the Gonads and Reproductive Tract

Development of the female reproductive tract involves cellular differentiation, migration, fusion, and canalization with probable apoptosis (programmed cell death). This complex and integrated sequence of events is associated with many opportunities for abnormal development and structural anomalies. Anomalies of the reproductive tract may manifest at different stages of life. Most abnormalities of the external genitalia are obvious at birth, whereas obstructive and nonobstructive lesions of the reproductive tract may be apparent at birth or only later: during childhood, at puberty, in adolescence, or in adulthood (10).

## Structural Anomalies of the Reproductive Tract

Reproductive tract anomalies may result from agenesis and/or hypoplasia or abnormalities related to lateral fusion, vertical fusion, or resorption. Although various classifications of these anomalies have been proposed, each has its limitations, and none is comprehensive. The American Society for Reproductive Medicine, or ASRM, system separates the anomalies into groups with similar clinical manifestations and prognosis (Table 1, Fig E1 [online]). Vaginal anomalies are not addressed. The Vagina Cervix Uterus Adnexa–associated Malformations classification includes abnormalities not found in the ASRM classification (Table 2).

**Published online**
10.1148/radiol.13121724 **Content codes:** GU PD US

**Radiology 2014;** 270:644–657

**Abbreviations:**
DSD = disorders of sex development
PCOS = polycystic ovarian syndrome

Conflicts of interest are listed at the end of this article.

**Figure 1**

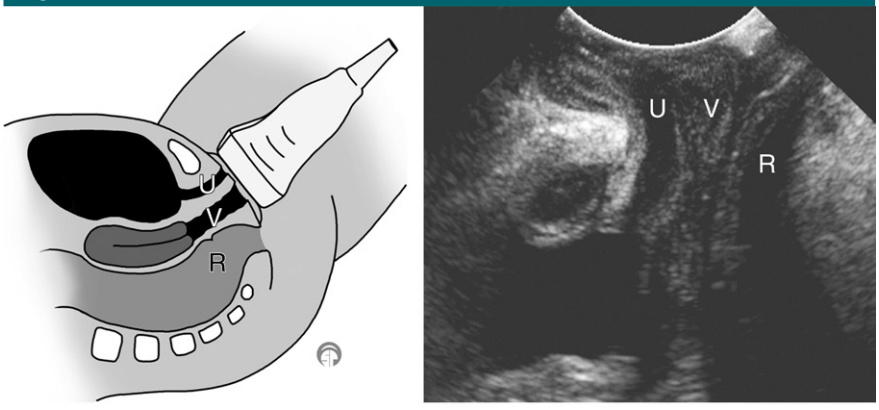


a. b.

**Figure 1:** Images depict transducer placement and normal female anatomy at transperineal US. **(a)** Sagittal diagram shows placement of a linear-array transducer on the perineum. **(b)** Corresponding sagittal transperineal US image. *R* = rectum, *U* = urethra, *V* = vagina.

**Figure 2**

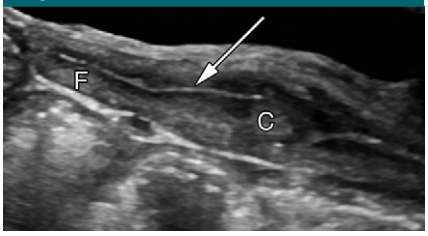


**Figure 2:** Sagittal US image of the neonatal uterus demonstrates that the anteroposterior diameter of the cervix *(C)* is greater than that of the fundus *(F)*. The endometrial cavity is visible as a thin, echogenic stripe in the center of the uterus (arrow).

**Figure 4**

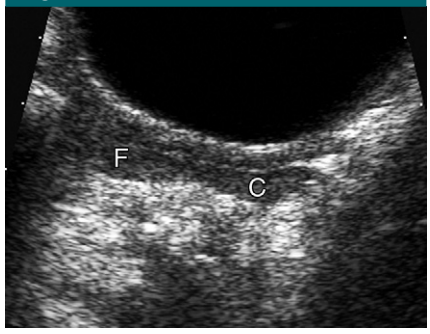


**Figure 4:** Sagittal US image of the uterus in a 7-year-old girl shows a cervix *(C)* that is comparable in thickness to the fundus *(F)*.

**Figure 3**

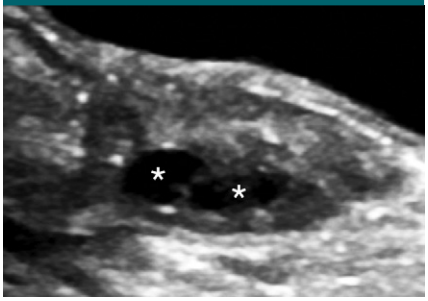


**Figure 3:** Sagittal US image of an ovary in an 11-month-old infant shows normal follicles (*).

**Table 1**

**Classification of Müllerian Anomalies according to the American Society for Reproductive Medicine System**

| Anomaly Type | Classification |
|---|---|
| Type I | "Müllerian" agenesis or hypoplasia |
| | A. Vaginal (uterus may be normal or exhibit a variety of malformations) |
| | B. Cervical |
| | C. Fundal |
| | D. Tubal |
| | E. Combined |
| Type II | Unicornuate uterus |
| | A. Communicating (endometrial cavity present) |
| | B. Noncommunicating (endometrial cavity present) |
| | C. Horn without endometrial cavity |
| | D. No rudimentary horn |
| Type III | Uterus didelphys |
| Type IV | Uterus bicornuate |
| | A. Complete (division down to internal os) |
| | B. Partial |
| Type V | Septate uterus |
| | A. Complete (septum to internal os) |
| | B. Partial |
| Type VI | Arcuate |
| Type VII | Diethylstilbestrol -related anomalies |
| | A. T-shaped uterus |
| | B. T-shaped uterus with dilated horns |
| | C. Uterine hypoplasia |

Note.—Reprinted, with permission, from references 11–13.

An imperforate hymen is the most common anomaly of the female reproductive tract. There are usually no other associated abnormalities. A diagnosis can be assigned at birth, when a bulge from the associated hydrocolpos and/or mucocolpos is present, owing to vaginal secretions related to maternal estrogen stimulation. If not diagnosed at birth, the mucus will be resorbed, and the bulge will resolve. After the onset of menarche, the adolescent patient may be asymptomatic or have a history of cyclical abdominal and/or pelvic pain (10). A diagnosis of imperforate hymen can usually be made on the basis of physical examination alone. However, in many patients a complete physical examination is not performed at birth, and, frequently, cases in symptomatic adolescents are misdiagnosed initially (15). US shows fluid distension of the vagina and a lesser degree of uterine distension. Echogenic debris within the fluid is due to mucous secretions in neonates (Fig 5) and blood in postmenarcheal girls. Spillage of secretions through the fallopian tubes may lead to ascites.

Uterine and vaginal anomalies may be diagnosed in the neonatal period in girls who are undergoing evaluation of multiple congenital anomalies or in adolescence, during investigation of amenorrhea, mass, and pelvic and/or abdominal pain. In the young child, an initial US study will usually suffice until puberty, at which time MR imaging is indicated for a more complete assessment. In the ado-

**Table 2**

**Vagina Cervix Uterus Adnexa–associated Malformations Classification**

| Anatomic Subgroup and Classification | Definition |
|---|---|
| Vagina (V) | |
| 0 | Normal |
| 1a | Partial |
| 1b | Complete hymenal atresia |
| 2a | Incomplete septate vagina < 50% |
| 2b | Complete septate vagina |
| 3 | Stenosis of the introitus |
| 4 | Hypoplasia |
| 5a | Unilateral atresia |
| 5b | Complete atresia |
| S1 | Sinus urogenitalis (deep confluence) |
| S2 | Sinus urogenitalis (middle confluence) |
| S3 | Sinus urogenitalis (high confluence) |
| C | Cloacae |
| + | Other |
| # | Unknown |
| Cervix (C) | |
| 0 | Normal |
| 1 | Duplex cervix |
| 2a | Unilateral atresia and/or aplasia |
| 2b | Bilateral atresia and/or aplasia |
| + | Other |
| # | Unknown |
| Uterus (U) | |
| 0 | Normal |
| 1 | Arctuate |
| 1b | Septate < 50% of the uterine cavity |
| 1c | Septate > 50% of the uterine cavity |
| 2 | Bicornuate |
| 3 | Hypoplastic uterus |
| 4a | Unilaterally rudimentary or aplastic |
| 4b | Bilaterally rudimentary or aplastic |
| + | Other |
| # | Unknown |
| Adnexa (A) | |
| 0 | Normal |
| 1a | Unilateral tubal malformation, ovaries normal |
| 1b | Bilateral tubal malformation, ovaries normal |
| 2a | Unilateral hypoplasia and/or gonadal streak (including tubal malformation, if appropriate) |
| 2b | Bilateral hypoplasia and/or gonadal streak (including tubal malformation, if appropriate) |
| 3a | Unilateral aplasia |
| 3b | Bilateral aplasia |
| + | Other |
| # | Unknown |
| Associated malformation (M) | |
| 0 | None |
| R | Renal system |
| S | Skeleton |
| C | Cardiac |
| N | Neurologic |

Table 2 (continues)

lescent patient, MR imaging is generally performed after identification of abnormal US findings to conduct a complete evaluation of the genitourinary tract.

During normal development of the uterus, a resorption failure in the septum between the two embryological müllerian ducts results in a *septate* uterus. The external surface of the uterus has either a normal configuration or a flat, broad fundus, and there are two endometrial cavities. The septum can be partial or complete, in which case it extends to the internal cervical os. There is usually a single cervix (Fig 6). A *bicornuate* uterus results from partial nonfusion of the müllerian ducts. The uterine horns are not fully developed. The external surface is deeply indented, and the central myometrium may extend to the level of the internal cervical os (bicornuate unicollis) or external cervical os (bicornuate bicollis) (Fig 7). Complete nonfusion of both müllerian ducts leads to a *didelphys* uterus. The individual horns are fully developed and almost normal in size. Two cervices are inevitably present. A longitudinal or transverse vaginal septum may be noted. Didelphys uteri have the highest association with transverse vaginal septa, but septa may be observed with the other müllerian duplication anomalies, as well. A *unicornuate* uterus is a single horned uterus with a single round ligament and fallopian tube that occurs when there is complete or near-complete arrested development of one müllerian duct. In most of these patients, arrest is incomplete, and a contralateral rudimentary horn with or without functioning endometrium is present. The unicornuate uterus communicates with a single cervix and a normal vagina. The rudimentary horn may or may not communicate with the developed uterine horn. US may demonstrate two uterine horns of different sizes. No treatment is required, unless functional endometrium within a noncommunicating horn leads to hematometra or endometriosis (10,16,17).

A transverse vaginal septum results from a fusion and/or canalization failure in the müllerian ducts and embryological urogenital sinus. In these patients, the external genitalia appear normal. A

**Table 2 (continued)**

**Vagina Cervix Uterus Adnexa–associated Malformations Classification**

| Anatomic Subgroup and Classification | Definition |
|---|---|
| + | Other |
| # | Unknown |

Note.—Reprinted, with permission, from reference 14.

**Figure 5**

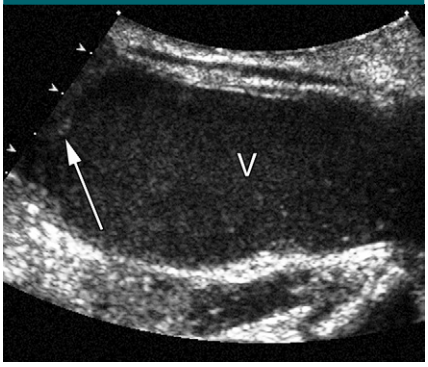


**Figure 5:** Imperforate hymen. Sagittal US image of the pelvis in a 1-day-old neonate shows a markedly distended vagina *(V)* filled with echogenic fluid. A portion of the cervix is visible superiorly (arrow).

**Figure 6**

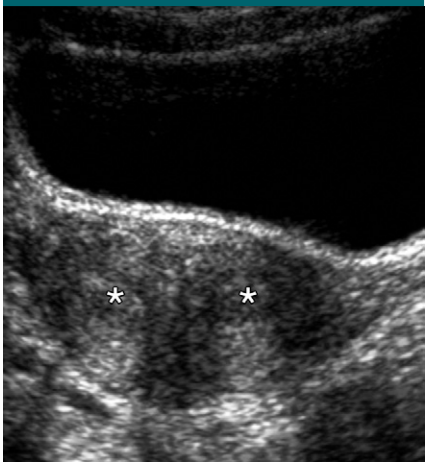


**Figure 6:** Septate uterus. Transverse US image of the uterus in a 16-year-old girl with pelvic pain and severe menstrual cramping demonstrates two separate endometrial cavities (*). The external myometrial contour is normal (see Movies 1a and 1b [online]).

**Figure 7**

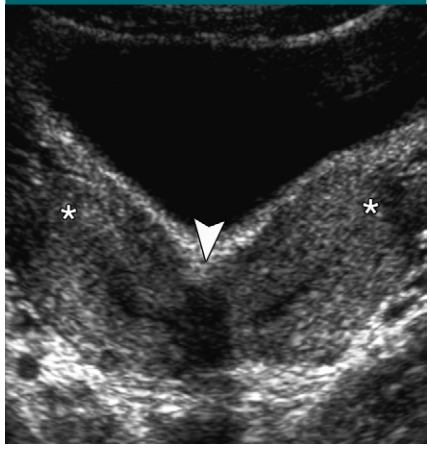


**Figure 7:** Bicornuate uterus in an 11-year-old girl with severe dysfunctional uterine bleeding. Transverse US image shows two uterine horns (*) separated by a central indentation (arrowhead) (see Movie 2 [online]).

**Figure 8**

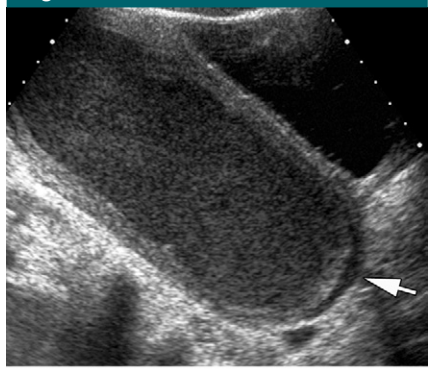

a.

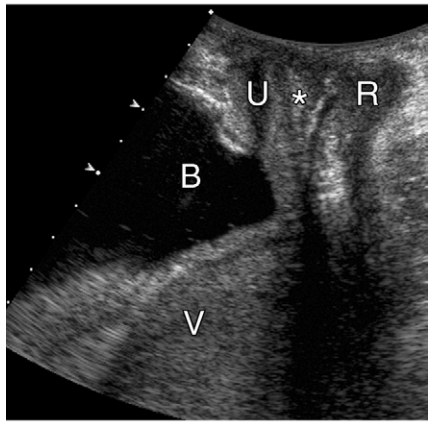


b.

**Figure 8:** Transverse vaginal septum. **(a)** Sagittal US image of the pelvis in a 12-year-old girl with normal external genitalia shows marked distension of the uterus and upper vagina with blood and secretions. A hypoechoic crescent of tissue at the most inferior aspect of the dilated upper vagina represents the vaginal septum (arrow). **(b)** Sagittal transperineal US image demonstrates a collapsed distal vagina (*). The septum is not depicted on this view. *B* = bladder, *R* = rectum, *U* = urethra, *V* = dilated proximal vagina.

complete vaginal septum may be located in the upper (46%), middle (40%), or lower (14%) vagina (18). The vagina is short or is a blind-ending pouch. The septa are generally less than 1 cm in thickness and extend completely or incompletely across the vagina (Fig 8). There is often a small central or eccentric perforation. Patients may present with mucocolpos in infancy or childhood, hematocolpos in adolescence, and/or pyohematocolpos due to ascending infection that occurs through the small perforation. It is clinically important to identify a cervix at imaging examination to differentiate between a high vaginal septum and cervical atresia, since treatment and prognosis differ (10).

Cervical atresia is rare and occurs in association with absence of the upper vagina. Patients may present with primary amenorrhea, cyclic or chronic abdominal or pelvic pain, or a pelvic mass. The usual treatment is hysterectomy.

Müllerian aplasia, also known as vaginal agenesis and Mayer-Rokitansky-Küster-Hauser syndrome, is the congenital absence of the vagina in association with variable müllerian duct anomalies. The incidence is approximately 1 in 5000 female births (17). There is usually associated cervical and uterine agenesis, although about 7%–10% of patients have a normal but obstructed uterus, an

**Figure 9**

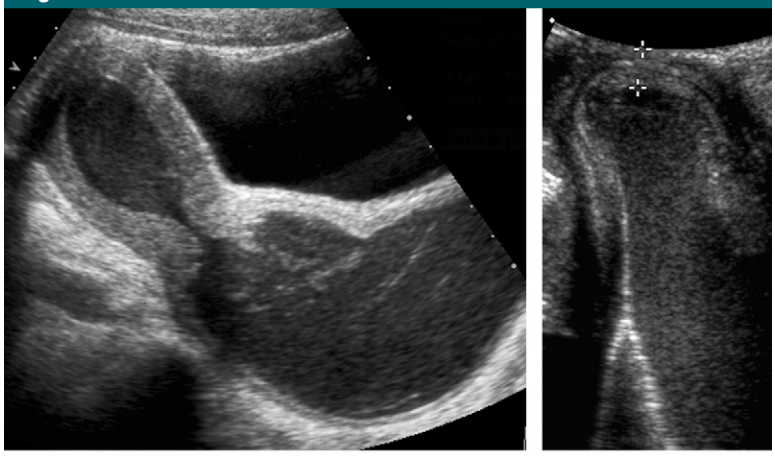

a. b.

**Figure 9:** Distal vaginal atresia in a 15-year-old girl with no vaginal orifice. **(a)** Sagittal US image of the pelvis demonstrates a dilated uterus and upper vagina filled with blood and secretions. **(b)** Sagittal transperineal US image used to measure the distance (between calipers) from the perineum to the obstructed, fluid-filled vagina. There is no vaginal tissue distal to the obstruction.

**Table 3**

**DSD Definitions**

| Disorder | Definition |
|---|---|
| Sex chromosome DSD | 45,X and 46,XY mixed gonadal dysgenesis; 46,XX and 46,XY chimerism |
| 46,XX DSD (chromosomally female) | Defect in ovarian development; disorder leading to high levels of androgens (congenital adrenal hyperplasia most common); abnormality of müllerian ducts (dysgenesis or hypoplasia), uterus, or vagina |
| 46,XY DSD (chromosomally male) | Defect in testicular development; disorder of androgen synthesis or action; syndrome associated with defects in genital development (cloacal anomaly, genetic syndrome, vanishing testis syndrome, congenital hypogonadotropic hypogonadism) |

obstructed septate uterus, or a rudimentary uterus with functional endometrium (17). Auditory, renal, and skeletal anomalies occur in a substantial proportion of patients. Affected individuals have a normal female 46,XX karyotype with normal ovarian hormonal and oocyte function. At physical examination, patients exhibit normal secondary sexual characteristics and a normal perineum. The hymen is usually present, along with a small distal vaginal pouch or vaginal dimple, since the hymen and distal vagina are both derived embryologically from the urogenital sinus. US is performed to confirm the presence of normal ovaries, to characterize any müllerian tissue, and to determine renal presence, position, and morphology.

Distal vaginal atresia occurs when the lower portion of the vagina fails to develop from the urogenital sinus and fibrous tissue replaces the absent distal vagina. The uterus, cervix, and upper vagina are normal. Affected individuals usually present with primary amenorrhea and may develop cyclical or chronic pain and a pelvic or abdominal mass as the upper vagina becomes distended with blood and secretions. Patients have normal secondary sexual characteristics. However, a vaginal orifice is absent. Transperineal US is useful in documenting absence of the distal vagina and measuring the distance between the proximal vagina and the perineal surface, particularly in an intraoperative setting (10) (Fig 9).

## Ambiguous Genitalia

Although a child born with ambiguous genitalia is a rare event, the potential psychological damage to the patient and his or her family that is caused by a delayed or incorrect diagnosis warrants the need for some familiarity of the underlying origins and the initial approach to diagnosis and management on the part of healthcare providers. Any deviation from the normal appearance of the genitalia, such as labial fusion or clitoromegaly, should prompt immediate investigation.

In 2006, the Lawson Wilkins Pediatric Endocrine Society and the European Society for Pediatric Endocrinology organized an International Consensus Conference on Intersex and published a consensus statement proposing the term *disorders of sex development* (DSD) to indicate congenital conditions with atypical development of chromosomal, gonadal, or anatomic sex (19). The DSDs are classified as sex chromosome DSD (karyotype is not the usual 46,XX or 46,XY); 46,XX DSD (chromosomally female); and 46,XY DSD (chromosomally male) (Table 3). Karyotyping, hormonal analysis, and imaging evaluation are required for proper characterization of these disorders.

US is used to determine the location of the gonads and the presence of a uterus and to assess the adrenal glands for diffuse enlargement or masses. A retrograde genitogram, obtained by injecting contrast material through the urogenital orifice (Fig 10), and/or a voiding cystourethrogram will delineate the anatomy of the urethra, vagina (if present), urogenital sinus, and occasionally the cervix. In the setting of a cloacal anomaly, delineation of the connections of the urinary, genital, and

**Figure 10**

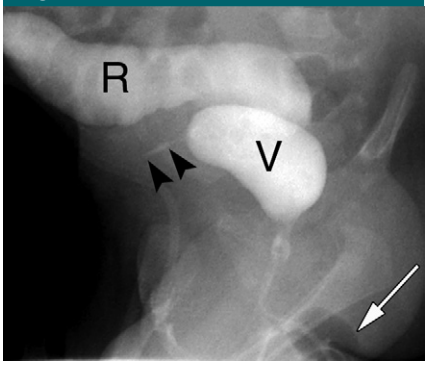


**Figure 10:** Sagittal oblique image from retrograde genitography in a 2.5-month-old infant with a cloacal malformation. A Foley catheter was placed into the perineal opening, and the balloon was inflated on the perineum (arrow). Contrast material injected through the catheter fills the vagina *(V)* and rectum *(R)*. A small amount of contrast material outlines the endocervical canal (arrowheads).

**Figure 11**

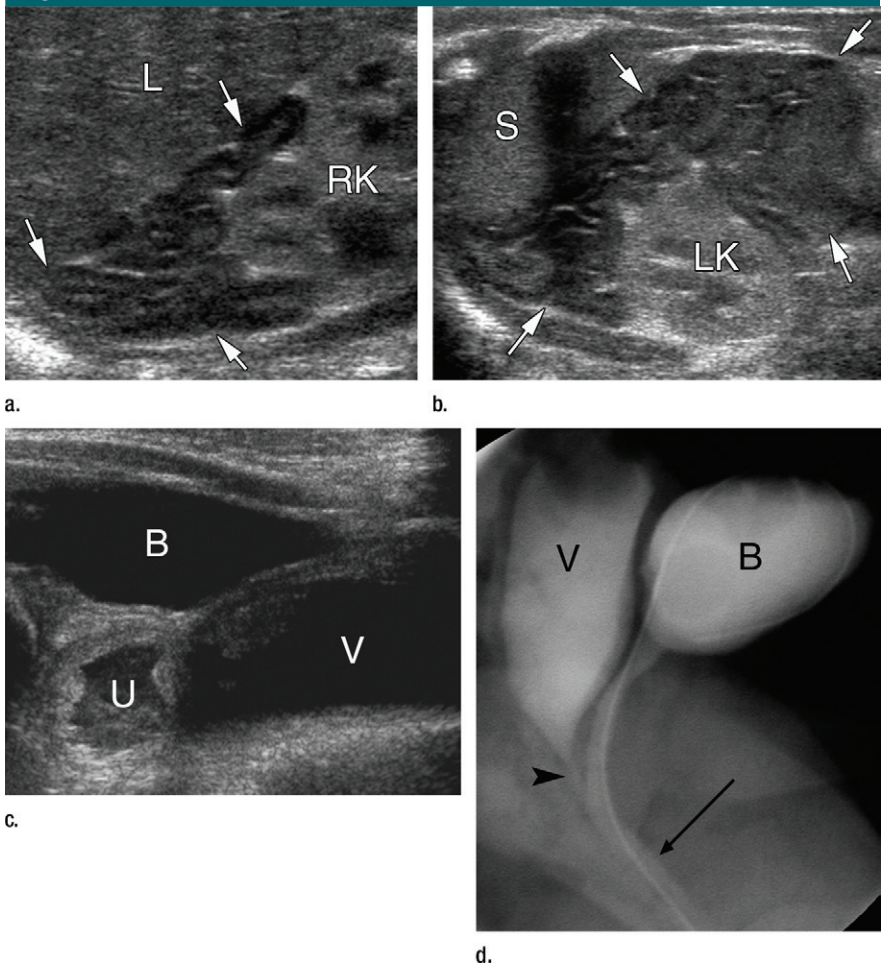


**Figure 11:** Adrenal hyperplasia in a 6-month-old infant with clitoromegaly. **(a, b)** Transverse US images demonstrate markedly enlarged, cerebriform right (**a**) and left (**b**) adrenal glands (between arrows). **(c)** Sagittal US image of the pelvis shows a dilated, fluid-filled vagina and uterus. **(d)** Sagittal image from voiding cystourethrography shows a catheter coiled within the bladder. There is reflux of urine into the vagina that communicates with the urogenital sinus (arrow) via a short channel (arrowhead). *B* = bladder, *L* = liver, *LK* = left kidney, *RK* = right kidney, *S* = spleen, *U* = uterus, *V* = vagina.

gastrointestinal tracts to the cloaca can also be ascertained (20,21).

The most common cause of sex chromosome DSD is 45,X (Turner syndrome), caused by absence of part or all of one of the X chromosomes. Monosomy X is the most common. Associated abnormalities include Hashimoto thyroiditis, congenital heart disease, renal anomalies, diabetes, and skeletal abnormalities. Characteristic physical features include short stature, low-set ears, webbed neck, and broad chest. Gonadal dysfunction manifests as amenorrhea and sterility. US demonstrates a juvenile appearance of the uterus, and the ovaries may not be visualized (Fig E2 [online]).

Most cases of 46,XX DSD are caused by congenital adrenal hyperplasia. In these patients, the adrenal glands are enlarged, and there is masculinization of the lower urogenital tract. Reflux of urine into the vagina and uterus in patients with a urogenital sinus can lead to hydrometrocolpos. The uterus and ovaries are normal (Fig 11). Rarer causes of masculinized but chromosomally normal females include maternal androgen ingestion in early pregnancy and a masculinizing ovarian tumor.

A cloacal malformation occurs as a result of interruption of the normal differentiation of the urinary, genital, and gastrointestinal tracts. Cloacal malformations occur exclusively in females, with an incidence of 1 in 40000 to 50000 newborns. Failure of the urorectal septum to form or fuse properly during embryological development results in incomplete separation of these tracts with a common confluence, the cloaca, and a single perineal orifice. There is usually an associated fusion failure in the müllerian ducts that leads to duplication of the uterus and proximal vagina. The urogenital sinus persists, and the hymen and lower vagina do not form appropriately. Drainage of pooled urine through the vagina is generally necessary to prevent bladder outlet obstruction, and the gastrointestinal tract is decompressed with a colostomy. Many of these children have additional congenital anomalies and often require multiple reconstructive operations. Detailed diagnosis usually requires genitography and/or voiding cystourethrography (Fig 12), as well as con-

**Figure 12**

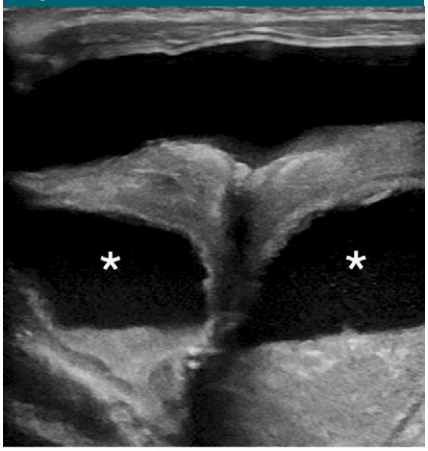


a.

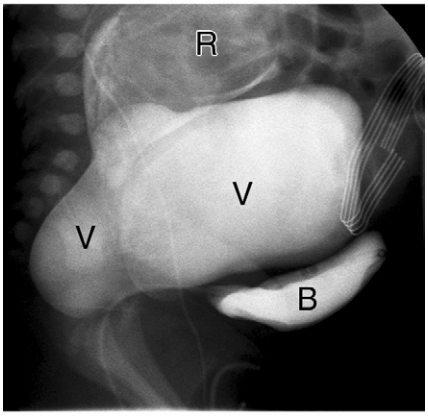


b.

**Figure 12:** Images in a 4-day-old neonate with cloacal malformation. **(a)** Transverse US image of the pelvis shows duplicated vaginas filled with fluid and debris (*). **(b)** Sagittal image from voiding cystourethrography shows a catheter in the bladder *(B)*. Contrast material has refluxed into both vaginas *(V)*, as well as into the rectum *(R)*, which communicates with the cloaca in the midline, between the duplicated vaginas. (Image courtesy of Jeanne S. Chow, MD, Boston Children's Hospital and Harvard Medical School, Boston, Mass.)

trast material–enhanced examination of the distal limb of the colostomy (10,20).

## Prepubertal Bleeding

Vulvovaginitis is the most common origin of prepubertal bleeding. Other underlying abnormalities include precocious puberty, vaginal foreign body, genital trauma (accidental trauma, self-inflicted trauma, or trauma resulting from physical or sexual abuse), and a vaginal mass.

**Figure 13**

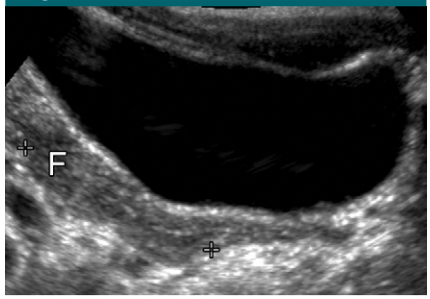


a.

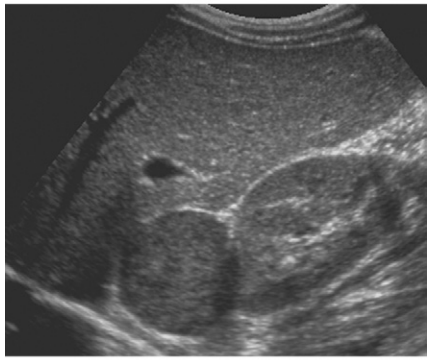

b.

**Figure 13:** Adrenocortical carcinoma in a 6-year-old girl, with early development of pubic hair, axillary odor, clitoromegaly, and hypertension. **(a)** Sagittal US image of the pelvis shows a peripubertal appearance of the uterus (between cursors), with relative prominence of the uterine fundus *(F)*. **(b)** Sagittal US image of the right adrenal gland depicts a large, solid adrenal mass. The child died several years later of metastatic disease.

## Precocious Puberty

The definition of precocious puberty in North American girls is somewhat controversial. However, the traditional definition of breast or pubic hair development in girls younger than 8 years of age is still used by most endocrinologists. Precocious puberty may be central and gonadotropin dependent in origin or peripheral and gonadotropin independent in origin. There are also incomplete forms of precocious puberty, including premature thelarche (breast development), premature pubarche (adrenarche; pubic or axillary hair), and isolated premature menarche without other signs of puberty (22).

In central precocious puberty, activation of the hypothalamic-pituitary-gonadal axis with secretion of gonadotropin-releasing hormone by the hypothalamus leads to isosexual pubertal development. Although the cause of central precocious puberty in most patients (>80%) is idiopathic, lesions of the hypothalamus, pituitary gland, or adjacent structures have been identified at CT and MR imaging. Central nervous system abnormalities that lead to precocious puberty can occur at any time during childhood, although they are more common in younger children. Some authors therefore recommend that all girls younger than 8 years of age who have progressive central precocity undergo central nervous system imaging (23). Prolonged exposure to sex steroids from any source can also trigger central precocious puberty (22).

In gonadotropin-independent (peripheral) precocious puberty, serum gonadotropin levels are low. An ovarian cyst or tumor, or, occasionally, an adrenal tumor, may produce estrogen autonomously. These lesions often produce high levels of estrogen, and pubertal development may progress more rapidly than in children with central precocity. Girls exposed to topical or ingested androgen or estrogen can also develop signs of precocity, such as virilization or breast development (22). US is used to assess ovarian size and morphology and to confirm or exclude a postpubertal appearance of the internal genitalia. US can be used to diagnose an estrogen-secreting adrenal or ovarian tumor and is used to monitor the effect of medical or surgical treatment (Fig 13).

## Vaginal Foreign Body

Toilet paper and fibrous material from clothing and carpets are the most common vaginal foreign bodies. Other causes include self-exploration and sexual abuse. Patients may present with vaginal bleeding, discharge, urinary symptoms, and abdominal or pelvic pain. With US, both radiopaque

**Figure 14**

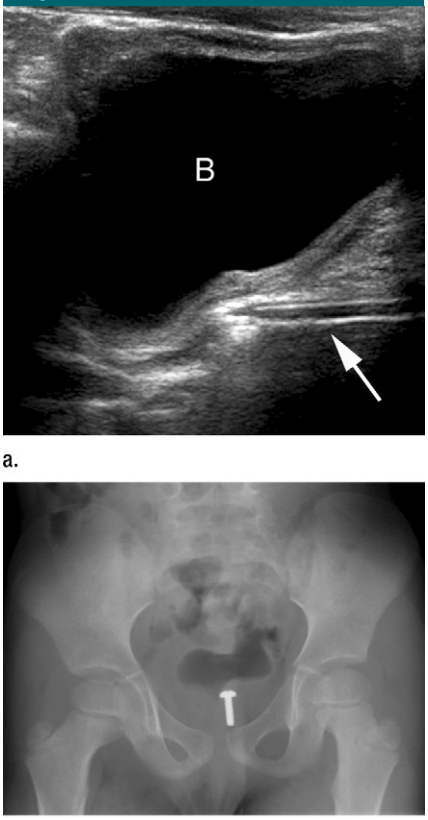


a.



b.

**Figure 14:** Images of a vaginal foreign body in a 4-year-old girl. **(a)** Sagittal US image demonstrates a tubular foreign body (arrow) indenting the posterior wall of the bladder *(B)*. **(b)** Anteroposterior supine radiograph shows a screw in the midpelvis that was removed at vaginoscopy.

**Figure 15**

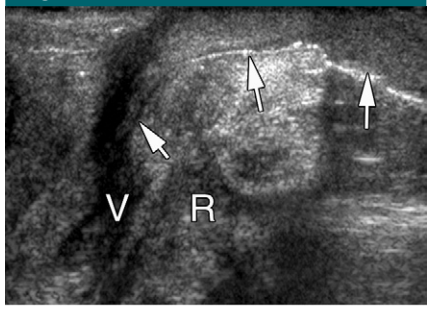


a.

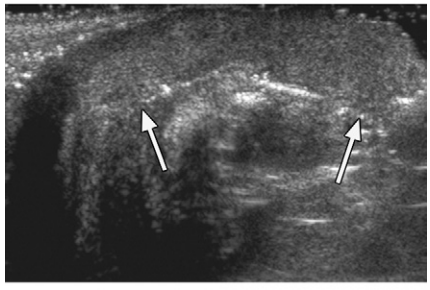

b.

**Figure 15:** Fibroepithelial polyp in a 17-year-old girl with a protruding vaginal mass. **(a, b)** Sagittal transperineal US images demonstrate a solid mass (arrows) protruding through the vaginal lumen *(V)*, anterior to the rectum *(R)*.

**Figure 16**

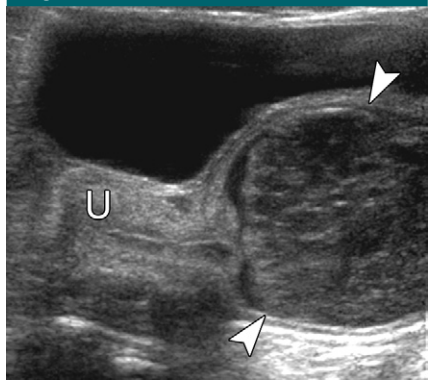


**Figure 16:** Vaginal rhabdomyosarcoma in a 16-month-old girl with a mass protruding through the introitus. Sagittal US image of the pelvis demonstrates a large soft-tissue mass within the vaginal lumen (between arrowheads). The uterus *(U)* appears normal.

and nonradiopaque objects can appear echogenic. Distal acoustic shadowing can be present, and there may be a slight indentation on the posterior bladder wall (2,24) (Fig 14).

### Vaginal Masses

Benign vaginal masses include cysts and polyps (Fig 15, Fig E3 [online]). Malignant masses are rare and include rhabdomyosarcoma, endodermal sinus tumor, and clear cell carcinoma (25–29).

Vaginal rhabdomyosarcoma arises in the anterior wall adjacent to the cervix. Uterine involvement occurs secondary to direct extension of tumor from the vagina. Patients may have vaginal bleeding and a vaginal, vulvar, or perineal mass. The tumor has a bimodal distribution, with the first peak between 2 and 6 years of age and the second between 14 and 18 years of age. The embryonal and botryoid subtypes are the most common. Tumors metastasize to the liver, lymph nodes, lung, and bone (Fig 16, Fig E4 [online]). US is often the first imaging modality used in the work up of girls with vaginal rhabdomyosarcoma. MR imaging or CT is required to assess the full extent of pelvic disease, and chest CT is performed to determine the presence of pulmonary metastases.

### Primary Amenorrhea

Fewer than 10% of girls have menarche before age 11, while 90% have begun to menstruate by age 13.75 years (30,31). Absence of menarche by the age of 15 years is termed "primary amenorrhea." Causes of primary amenorrhea include gonadal dysgenesis (50%); hypothalamic hypogonadism (20%); absence of the uterus, cervix, and/or vagina (15%); transverse vaginal septum or imperforate hymen (5%); pituitary disease (5%); and other disorders (polycystic ovarian syndrome [PCOS]; congenital adrenal hyperplasia; androgen insensitivity) (5%) (32). US is usually the initial imaging study performed in the evaluation of these patients. The need for additional imaging studies is dictated by the associated abnormalities.

PCOS is the most common endocrinopathy in premenopausal women, affecting 6%–8% of females of reproductive age (33). Despite its high prevalence, the diagnostic criteria and treatment are not universally agreed upon. The Androgen Excess Society criteria for PCOS include *(a)* hyperandrogenism (hirsutism and/or hyperandrogenemia) and *(b)* ovarian dysfunction (oligoanovulation and/or polycystic ovaries at US) (34). The diagnosis of PCOS in young adolescents is especially challenging, since transient oligomenorrhea and mild hyperandrogenemia are common in the first few years after the onset of menarche.

The sonographic features of PCOS are variable; the ovaries may appear normal or enlarged, with multiple

**Figure 17**

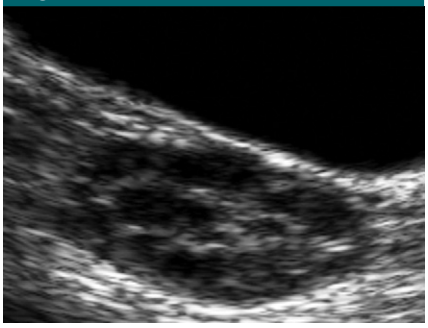

**Figure 17:** Polycystic ovarian syndrome in an 11-year-old girl with secondary amenorrhea. Sagittal US image of the right ovary (volume, 20.5 mL) demonstrates multiple, small intraparenchymal follicles with a predominantly peripheral distribution.

small follicles (Fig 17, Fig E5 [online]). The Rotterdam US criteria define polycystic ovaries as the presence of 12 or more follicles measuring 2 to 9 mm in diameter or an ovarian volume of more than 10 mL in at least one ovary, as measured at transvaginal US (35). Since most adolescent girls will undergo transabdominal US and not transvaginal US, a determination of the number of ovarian follicles is difficult, and volume measurements are generally used as the main diagnostic criterion.

## Gynecologic Pelvic Masses

Gynecologic masses in girls include ovarian cyst, hematocolpos, primary ovarian neoplasm, metastatic ovarian disease, primary vaginal and uterine neoplasms, and pregnancy.

### Ovarian Masses

Ovarian masses include nonneoplastic cysts and benign and malignant tumors. Most tumors in the pediatric population are benign and of germ cell origin, unlike adults, where epithelial neoplasms predominate.

### Ovarian Cyst

Fetal ovarian cysts are occasionally detected at antenatal sonography. They are usually unilateral, and most are thought to result from ovarian stimulation by maternal and fetal gonadotropins. Ovarian cysts are often displaced into the abdomen, where they may be palpable and are simple or complex at US. Most are asymptomatic, and spontaneous regression occurs after birth. Regression usually occurs within 3–4 months but can take as long as a year (36). Serial US studies are performed to document regression.

**Figure 18**

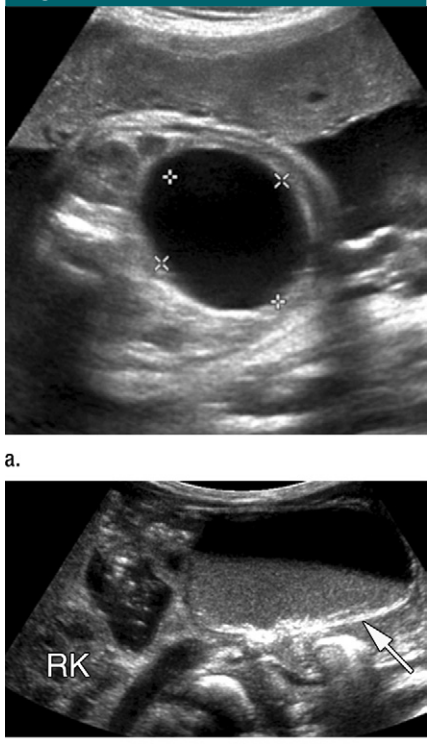


a.

b.

**Figure 18:** Prenatal ovarian cyst complicated by torsion. **(a)** Prenatal US image shows a simple ovarian cyst (between cursors). A large mass was palpable at birth. **(b)** Sagittal postnatal US image obtained at 10 days of age shows a cystic structure filled with layering debris extending out of the pelvis and into the abdomen (arrow). Ovarian torsion was subsequently identified at surgery. *RK* = right kidney.

The development of hemorrhage within an ovarian cyst in utero or postnatally has a high association with long-term ovarian loss, generally thought to be due to torsion (Fig 18), although there has been some speculation in the literature that the underlying origin may be related instead to ovarian dysgenesis (37,38). US features of hemorrhagic ovarian cysts reflect the age of the blood: Fresh blood is hyperechoic relative to the ovarian parenchyma, older blood has a heterogeneous appearance, and a blood clot undergoing lysis becomes anechoic.

In the prepubertal child, ovarian cysts may be functional or nonfunctional. Functional cysts develop as a result of gonadotropin stimulation of the ovary, with a decreased incidence in early childhood after the neonatal period and an increase as puberty is approached. Some functional cysts will be hormonally active and cause gonadotropin-independent (peripheral) precocious puberty, which manifests as premature breast development or vaginal bleeding. Nonfunctional ovarian cysts also occur in childhood and will appear as nonresolving cystic masses. Both types of cyst often appear as an asymptomatic abdominal mass or increasing abdominal girth noted by a parent or physician. Other modes of presentation include chronic abdominal pain, intermittent pain from torsion without complete compromise of the vascular supply, or acute, severe pain that mimicks appendicitis or peritonitis from hemorrhage, torsion, or perforation. Nonspecific symptoms, such as nausea, vomiting, bloating, urinary frequency, or retention, may also occur. US is used to document cyst size and to determine if a lesion is a simple cyst, a complex cyst, or a solid mass. Simple cysts or cysts with debris suggestive of hemorrhage are managed conservatively, with follow-up imaging examinations performed after 4–8 weeks to document regression. If the cyst persists at follow-up but the US features are reassuring, continued observation is appropriate. When a prepubertal simple ovarian cyst persists, increases in size to more than 5 cm in diameter, or is symptomatic, then surgery should be considered (39,40). Simple ovarian cysts and hemorrhagic corpus luteum cysts are common in postpubertal girls.

### Ovarian Tumors

Ovarian tumors may arise from germ cells, stroma, or surface epithelium. Most occur in the 2nd decade of life, with teratoma being the most common type.

Teratomas are composed of elements of all three germ cell layers: 90% are classified as mature or cystic, and 10% are classified as immature (containing embryonic neural elements) or malignant. Ectodermal components predominate in cystic teratomas, which are also known as dermoid cysts (41).

Cystic teratoma accounts for more than 90% of all benign ovarian tumors. It is usually unilateral, although 10%–20% are bilateral. Most tumors range from 5 to 10 cm in diameter. The US appearance depends on the relative amounts of sebum, serous fluid, calcium, hair, and fat within the lesion (29,42,43). Most tumors have a complex appearance and usually contain fewer than 50% soft-tissue elements by volume (Fig 19, Fig E6 [online]).

Malignant ovarian neoplasms are rare, accounting for only 1%–2% of all malignant neoplasms in children younger than 17 years of age (44–46). Malignant germ cell tumors usually occur in postmenarcheal girls and most often manifest as an asymptomatic pelvic or abdominal mass. They are typically larger than 10 cm in diameter at the time of diagnosis. Intraabdominal spread involves the lymph nodes and liver. Dysgerminoma is the most common ovarian malignancy in childhood; 10% are bilateral. Malignant teratoma contains more than 50% soft-tissue elements by volume. Other germ cell tumors may be homogeneous and echogenic at US or complex with cystic areas, due to hemorrhage (29,41–43).

Sex cord stromal tumors are low-grade malignancies that arise from granulosa theca cells and Sertoli cells of the embryonic gonad. They are diagnosed most often in prepubertal girls and are usually asymptomatic. Granulosa theca cell tumor may cause isosexual precocity due to estrogen production (Fig 20, Fig E7 [online]). Sertoli-Leydig cell tumor may cause virilization as a result of androgen production. At US, these tumors appear as heterogeneous masses with cystic foci. Metastases are unusual but may occur on the peritoneal surfaces or within the liver (29,41–43).

Epithelial tumors are rare before puberty; the most common types are serous and mucinous cystadenoma, most of which are benign (47). Serous cystadenoma is usually a large, unilocular, thin-walled cystic mass that may contain thin septations and papillary projections; approximately 20% are bilateral. Mucinous cystadenoma generally occurs as a large, multiloculated cystic mass. Papillary projections are identified less frequently, and it is less likely to be bilateral in comparison to serous cystadenoma (29,42).

Although little has been reported on the subject of metastatic ovarian tumors in children, the ovaries may serve as a sanctuary for leukemia (48), and metastatic spread from neuroblastoma, Burkitt lymphoma (49), colon cancer, and rhabdomyosarcoma (50) has been documented. Metastatic ovarian involvement is often asymptomatic, and diagnosis is only made at autopsy (51).

**Figure 19**

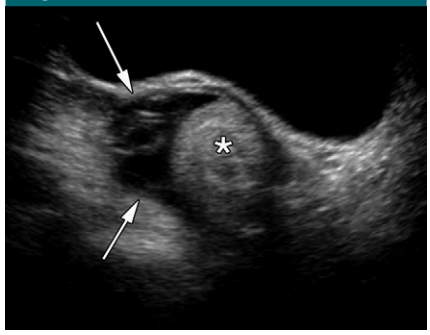

**Figure 19:** Ovarian dermoid cyst in a 14-year-old girl. Sagittal US image of the left adnexa demonstrates a complex mass that contains both cystic (arrows) and solid, echogenic (*) components.

**Figure 20**

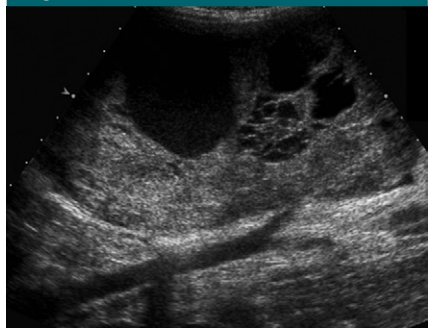

**Figure 20:** Granulosa theca cell tumor in a 9-year-old girl with breast development, vaginal bleeding, and abdominal pain. Sagittal US image demonstrates a large, solid mass of the abdomen and pelvis that contained cystic foci.

### Pregnancy

Pregnancy should be considered in the differential diagnosis of a pelvic mass in girls 9 years of age and older. There is an increased risk of complications in pediatric pregnancy, including toxemia, preeclampsia, placental abruption, laceration, and need for cesarean section (52).

## Pelvic Pain

Causes of pelvic pain include adnexal torsion, hemorrhagic ovarian cyst, pelvic inflammatory disease, ectopic pregnancy, and appendicitis.

### Adnexal (Ovarian and/or Tubal) Torsion

Partial or complete rotation of the ovary on its vascular pedicle compromises venous and lymphatic drainage, as well as arterial inflow. Torsion is nearly always unilateral, and pathologic findings range from massive edema to parenchymal necrosis. Ovarian torsion in neonates and premenarcheal girls is a rare event because most cases are related to the presence of an ovarian cyst, which is uncommon in this population. However, torsion of a normal adnexum can occur. Hypermobility due to lax supporting ligaments is thought to account for torsion of the normal adnexum. The peak incidence of adnexal torsion occurs in adolescence and young adulthood (53).

The affected ovary is always enlarged, with a median volume 12 times that of the contralateral normal ovary (54). Multiple mildly enlarged (8–12 mm), peripherally located follicles are the only relatively specific sign of torsion, believed to be caused by transudation of fluid as a result of vascular congestion (Fig 21). A ratio of torsed adnexal volume to normal adnexal volume that is higher than 20 is predictive of an associated ovarian mass, whereas a ratio of less than 20 is predictive of absence of an ovarian mass (54).

**Figure 21**

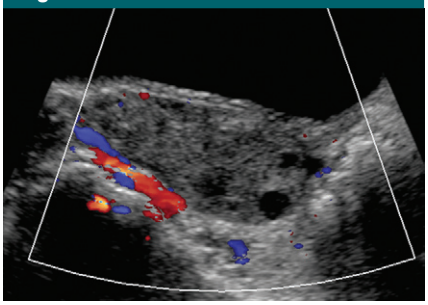

**Figure 21:** Adnexal torsion in a 5-year-old girl with acute onset of abdominal pain and nausea and a palpable pelvic mass. Color Doppler US image of the right adnexa shows an enlarged, avascular ovary with multiple peripheral follicles. Right ovarian volume was 27 mL, and left ovarian volume was 1.3 mL. There was no associated right ovarian mass at surgery.

**Figure 22**

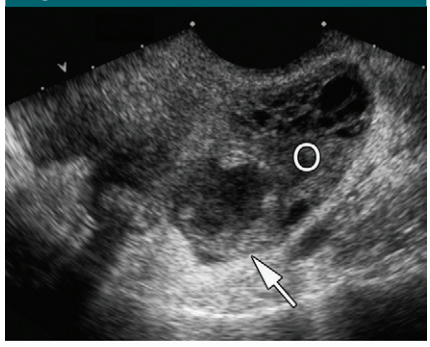

a.

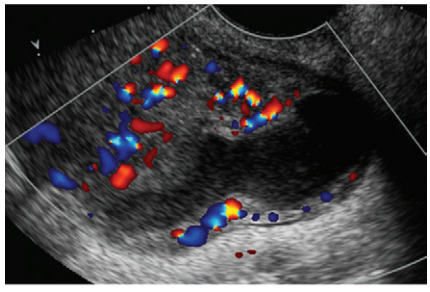

b.

**Figure 22:** Pyosalpinx in an 18-year-old woman with pelvic inflammatory disease. **(a)** Transvaginal US image shows a dilated, thick-walled fallopian tube (arrow) abutting the ovary *(O)*. The tube is filled with echogenic material. **(b)** Transvaginal color Doppler US image demonstrates mural hyperemia of the fallopian tube.

**Figure 23**

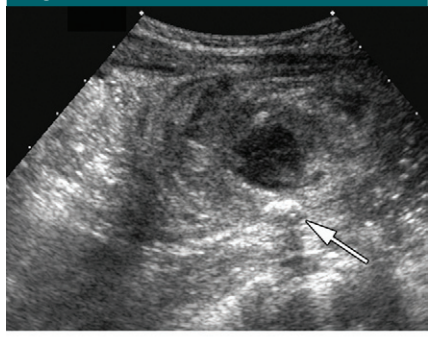

a.

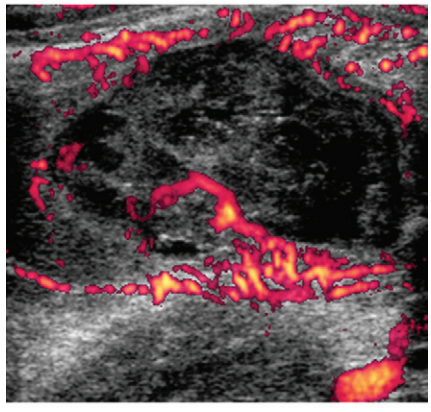

b.

**Figure 23:** Perforated appendicitis in a 3-year-old girl. **(a)** Sagittal US image of the right lower quadrant of the abdomen shows a well-circumscribed, heterogeneous collection with an echogenic focus at its base, associated with distal shadowing (arrow) in keeping with an appendicolith. **(b)** Color Doppler US image depicts prominent peripheral hyperemia, which is compatible with an abscess.

### Pelvic Inflammatory Disease

Pelvic inflammatory disease affects girls of reproductive age and is usually due to an ascending sexually transmitted infection. Common causative organisms include *Neisseria gonorrheae* and *Chlamydia trachomatis*. The diagnosis is generally established clinically on the basis of fever, pelvic pain, tenderness, and vaginal discharge (55).

US is useful in identifying complications of pelvic inflammatory disease, including pyosalpinx and tubo-ovarian abscess. USc findings depend on the stage of the inflammatory process: Findings are minimal, if any imaging abnormalities are detectable early in the course of infection. Pyosalpinx appears as either a thick-walled, fluid-filled tubular structure or as an oval or round mass with low-level echoes due to the presence of purulent debris (Fig 22). There is a spectrum of ovarian involvement, including enlargement and increased ovarian echogenicity; tubo-ovarian complex, consisting of an abnormal matting together of the ovary and fallopian tube; and tubo-ovarian abscess, resulting in a complex intraovarian mass (56).

### Ectopic Pregnancy

A complete discussion of ectopic pregnancy is beyond the scope of this article. However, it is important to note that it occurs on rare occasion in young adolescents who have the highest reported death rate. The diagnosis should be considered in the presence of pelvic pain, an abnormal serum β-human chorionic gonadotropin level, irregular vaginal bleeding, and a missed menstrual period (57).

### Acute Appendicitis

Acute appendicitis is the most common pediatric surgical emergency. Patients typically present with right lower quadrant pain, tenderness, and leukocytosis. Symptoms of acute appendicitis overlap with a number of other gastrointestinal conditions, including mesenteric adenitis and Crohn disease, as well as acute gynecologic conditions.

The appendix is optimally imaged with US by using a high-frequency transducer and a graded-compression technique. The inflamed appendix is depicted as a noncompressible, tubular, blind-ending structure that demonstrates a gut signature and an outer diameter larger than 6 mm (58). Intraluminal stones (appendicoliths), periappendiceal inflammation, and abscesses are also readily detected (Fig 23, Fig E8 [online]). Advantages of US for diagnosis relative to CT include lack of ionizing radiation; no need for contrast material administration or sedation, with the attendant risks; and lower cost.

In our practice, we will initially perform a US examination in patients suspected of having acute appendicitis. Cross-sectional imaging with CT or MR imaging is reserved for those patients in whom the appendix is not visualized at US, for patients in whom the US study

is equivocal and there is a strong clinical suspicion for acute appendicitis, or for patients in whom a perforated appendix is suspected on the basis of initial US imaging findings and a more complete assessment of inflammatory changes and fluid collections is desired for management purposes (59–61).

## Conclusion

As the main imaging modality for the pediatric female pelvis, US is useful in depicting ovarian and uterine anatomy; assessing the hormonal status of children with primary amenorrhea, ambiguous genitalia, prepubertal bleeding, and precocious puberty; and determining the origin of pelvic masses and the cause of pelvic pain.

**Disclosures of Conflicts of Interest: H.J.P.** Financial activities related to the present article: none to disclose. Financial activities not related to the present article: author received reimbursement of travel expenses paid out of her academic fund at the Department of Radiology, Boston Children's Hospital, to attend and make presentations at professional meetings. Other relationships: none to disclose. **A.P.** No relevant conflicts of interest to disclose.

## References

1. Garel L, Dubois J, Grignon A, Filiatrault D, Van Vliet G. US of the pediatric female pelvis: a clinical perspective. RadioGraphics 2001; 21(6):1393–1407.
2. Ziereisen F, Guissard G, Damry N, Avni EF. Sonographic imaging of the paediatric female pelvis. Eur Radiol 2005;15(7):1296–1309.
3. Stranzinger E, Strouse PJ. Ultrasound of the pediatric female pelvis. Semin Ultrasound CT MR 2008;29(2):98–113.
4. Coley BD. Pediatric gynecologic ultrasound. Ultrasound Clin 2012;7(1):107–121.
5. Teele RL, Share JC. Transperineal sonography in children. AJR Am J Roentgenol 1997; 168(5):1263–1267.
6. Orsini LF, Salardi S, Pilu G, Bovicelli L, Cacciari E. Pelvic organs in premenarcheal girls: real-time ultrasonography. Radiology 1984;153(1):113–116.
7. Cohen HL, Eisenberg P, Mandel F, Haller JO. Ovarian cysts are common in premenarchal girls: a sonographic study of 101 children 2-12 years old. AJR Am J Roentgenol 1992; 159(1):89–91.
8. Cohen HL, Shapiro MA, Mandel FS, Shapiro ML. Normal ovaries in neonates and infants: a sonographic study of 77 patients 1 day to 24 months old. AJR Am J Roentgenol 1993; 160(3):583–586.
9. Forrest TS, Elyaderani MK, Muilenburg MI, Bewtra C, Kable WT, Sullivan P. Cyclic endometrial changes: US assessment with histologic correlation. Radiology 1988;167(1): 233–237.
10. Laufer M. Structural abnormalities of the female reproductive tract. In: Emans SJ, Laufer MR, eds. Pediatric & adolescent gynecology. 6th ed. Philadelphia, Pa: Lippincott Williams & Wilkins, 2012; 188–237.
11. Buttram VC Jr. Müllerian anomalies and their management. Fertil Steril 1983;40(2): 159–163.
12. Buttram VC Jr, Gibbons WE. Müllerian anomalies: a proposed classification (an analysis of 144 cases). Fertil Steril 1979;32(1): 40–46.
13. The American Fertility Society classifications of adnexal adhesions, distal tubal occlusion, tubal occlusion secondary to tubal ligation, tubal pregnancies, Müllerian anomalies and intrauterine adhesions. Fertil Steril 1988; 49(6):944–955.
14. Oppelt P, Renner SP, Brucker S, et al. The VCUAM (Vagina Cervix Uterus Adnex-associated Malformation) classification: a new classification for genital malformations. Fertil Steril 2005;84(5):1493–1497.
15. Posner JC, Spandorfer PR. Early detection of imperforate hymen prevents morbidity from delays in diagnosis. Pediatrics 2005; 115(4):1008–1012.
16. Brody JM, Koelliker SL, Frishman GN. Unicornuate uterus: imaging appearance, associated anomalies, and clinical implications. AJR Am J Roentgenol 1998;171(5):1341–1347.
17. Junqueira BL, Allen LM, Spitzer RF, Lucco KL, Babyn PS, Doria AS. Müllerian duct anomalies and mimics in children and adolescents: correlative intraoperative assessment with clinical imaging. RadioGraphics 2009; 29(4):1085–1103.
18. Gibson ED. Transverse upper vaginal septum presenting in pregnancy: a case report and review of the literature. Aust N Z J Obstet Gynaecol 2003;43(5):381–383.
19. Lee PA, Houk CP, Ahmed SF, Hughes IA; International Consensus Conference on Intersex organized by the Lawson Wilkins Pediatric Endocrine Society and the European Society for Paediatric Endocrinology. Consensus statement on management of intersex disorders. Pediatrics 2006;118(2):e488–e500.
20. Jaramillo D, Lebowitz RL, Hendren WH. The cloacal malformation: radiologic findings and imaging recommendations. Radiology 1990;177(2):441–448.
21. Chavhan GB, Parra DA, Oudjhane K, Miller SF, Babyn PS, Pippi Salle FL. Imaging of ambiguous genitalia: classification and diagnostic approach. RadioGraphics 2008;28(7): 1891–1904.
22. Mansfield MJ. Precocious puberty. In: Emans SJ, Laufer MR, eds. Pediatric & adolescent gynecology. 6th ed. Philadelphia, Pa: Lippincott Williams & Wilkins, 2012; 114–124.
23. Carel JC, Léger JN. Clinical practice: precocious puberty. N Engl J Med 2008;358(22): 2366–2377.
24. Caspi B, Zalel Y, Katz Z, Appelman Z, Insler V. The role of sonography in the detection of vaginal foreign bodies in young girls: the bladder indentation sign. Pediatr Radiol 1995; 25(Suppl 1):S60–S61.
25. Tannous WN, Azouz EM, Homsy YL, Kiruluta HG, Grattan-Smith D. CT and ultrasound imaging of pelvic rhabdomyosarcoma in children: a review of 56 patients. Pediatr Radiol 1989;19(8):530–534.
26. Agrons GA, Wagner BJ, Lonergan GJ, Dickey GE, Kaufman MS. From the archives of the AFIP. Genitourinary rhabdomyosarcoma in children: radiologic-pathologic correlation. RadioGraphics 1997;17(4):919–937.
27. Wexler LH, Meyer WH, Helman LJ. Rhabdomyosarcoma and the undifferentiated sarcomas. In: Pizzo PA, Poplack DG, eds. Principles and practice of pediatric oncology. 5th ed. Philadelphia, Pa: Lippincott Williams & Wilkins, 2006; 971–1001.
28. Fernandez-Pineda I, Spunt SL, Parida L, Krasin MJ, Davidoff AM, Rao BN. Vaginal tumors in childhood: the experience of St. Jude Children's Research Hospital. J Pediatr Surg 2011;46(11):2071–2075.
29. Shah RU, Lawrence C, Fickenscher KA, Shao L, Lowe LH. Imaging of pediatric pelvic neoplasms. Radiol Clin North Am 2011; 49(4):729–748, vi.
30. Wu T, Mendola P, Buck GM. Ethnic differences in the presence of secondary sex characteristics and menarche among US girls: the Third National Health and Nutrition Examination Survey, 1988-1994. Pediatrics 2002;110(4):752–757.
31. Chumlea WC, Schubert CM, Roche AF, et al. Age at menarche and racial comparisons in US girls. Pediatrics 2003;111(1):110–113.

32. Reindollar RH, Byrd JR, McDonough PG. Delayed sexual development: a study of 252 patients. Am J Obstet Gynecol 1981;140(4):371–380.

33. Blank SK, Helm KD, McCartney CR, Marshall JC. Polycystic ovary syndrome in adolescence. Ann N Y Acad Sci 2008;1135:76–84.

34. Azziz R, Carmina E, Dewailly D, et al. Positions statement: criteria for defining polycystic ovary syndrome as a predominantly hyperandrogenic syndrome: an Androgen Excess Society guideline. J Clin Endocrinol Metab 2006;91(11):4237–4245.

35. Rotterdam ESHRE/ASRM-Sponsored PCOS consensus workshop group. Revised 2003 consensus on diagnostic criteria and long-term health risks related to polycystic ovary syndrome (PCOS). Hum Reprod 2004;19(1):41–47.

36. Kwak DW, Sohn YS, Kim SK, Kim IK, Park YW, Kim YH. Clinical experiences of fetal ovarian cyst: diagnosis and consequence. J Korean Med Sci 2006;21(4):690–694.

37. Enríquez G, Durán C, Torán N, et al. Conservative versus surgical treatment for complex neonatal ovarian cysts: outcomes study. AJR Am J Roentgenol 2005;185(2):501–508.

38. Ben-Ami I, Kogan A, Fuchs N, et al. Long-term follow-up of children with ovarian cysts diagnosed prenatally. Prenat Diagn 2010;30(4):342–347.

39. Laufer M. Adnexal masses. In: Emans SJ, Laufer MR, eds. Pediatric & adolescent gynecology. 6th ed. Philadelphia, Pa: Lippincott Williams & Wilkins, 2012; 381–404.

40. de Silva KS, Kanumakala S, Grover SR, Chow CW, Warne GL. Ovarian lesions in children and adolescents—an 11-year review. J Pediatr Endocrinol Metab 2004;17(7):951–957.

41. Amies Oelschlager AM, Sawin R. Teratomas and ovarian lesions in children. Surg Clin North Am 2012;92(3):599–613.

42. Epelman M, Chikwava KR, Chauvin N, Servaes S. Imaging of pediatric ovarian neoplasms. Pediatr Radiol 2011;41(9):1085–1099.

43. Anthony EY, Caserta MP, Singh J, Chen MY. Adnexal masses in female pediatric patients. AJR Am J Roentgenol 2012;198(5):W426–W431.

44. Barber HR. Ovarian cancer. CA Cancer J Clin 1986;36(3):149–184.

45. von Allmen D. Malignant lesions of the ovary in childhood. Semin Pediatr Surg 2005;14(2):100–105.

46. Brookfield KF, Cheung MC, Koniaris LG, Sola JE, Fischer AC. A population-based analysis of 1037 malignant ovarian tumors in the pediatric population. J Surg Res 2009;156(1):45–49.

47. Morowitz M, Huff D, von Allmen D. Epithelial ovarian tumors in children: a retrospective analysis. J Pediatr Surg 2003;38(3):331–335; discussion 331–335.

48. Kim JW, Cho MK, Kim CH, et al. Ovarian and multiple lymph nodes recurrence of acute lymphoblastic leukemia: a case report and review of literature. Pediatr Surg Int 2008;24(11):1269–1273.

49. Young RH, Kozakewich HP, Scully RE. Metastatic ovarian tumors in children: a report of 14 cases and review of the literature. Int J Gynecol Pathol 1993;12(1):8–19.

50. McCarville MB, Hill DA, Miller BE, Pratt CB. Secondary ovarian neoplasms in children: imaging features with histopathologic correlation. Pediatr Radiol 2001;31(5):358–364.

51. Siegel MJ. Female pelvis. In: Pediatric sonography. 4th ed. Philadelphia, Pa: Lippincott Williams & Wilkins, 2011; 527.

52. Black AY, Fleming NA, Rome ES. Pregnancy in adolescents. Adolesc Med State Art Rev 2012;23(1):123–138.

53. Rossi BV, Ference EH, Zurakowski D, et al. The clinical presentation and surgical management of adnexal torsion in the pediatric and adolescent population. J Pediatr Adolesc Gynecol 2012;25(2):109–113.

54. Servaes S, Zurakowski D, Laufer MR, Feins N, Chow JS. Sonographic findings of ovarian torsion in children. Pediatr Radiol 2007;37(5):446–451.

55. Shrier LA. Sexually transmitted infections: chlamydia, gonorrhea, pelvic inflammatory disease, and syphilis. In: Emans SJ, Laufer MR, eds. Pediatric and adolescent gynecology. 6th ed. Philadelphia, Pa: Lippincott Williams & Wilkins, 2012; 325–348.

56. Cicchiello LA, Hamper UM, Scoutt LM. Ultrasound evaluation of gynecologic causes of pelvic pain. Obstet Gynecol Clin North Am 2011;38(1):85–114.

57. Vichnin M. Ectopic pregnancy in adolescents. Curr Opin Obstet Gynecol 2008;20(5):475–478.

58. Jeffrey RB Jr, Laing FC, Townsend RR. Acute appendicitis: sonographic criteria based on 250 cases. Radiology 1988;167(2):327–329.

59. Krishnamoorthi R, Ramarajan N, Wang NE, et al. Effectiveness of a staged US and CT protocol for the diagnosis of pediatric appendicitis: reducing radiation exposure in the age of ALARA. Radiology 2011;259(1):231–239.

60. Thirumoorthi AS, Fefferman NR, Ginsburg HB, Kuenzler KA, Tomita SS. Managing radiation exposure in children—reexamining the role of ultrasound in the diagnosis of appendicitis. J Pediatr Surg 2012;47(12):2268–2272.

61. Hennelly KE, Bachur R. Appendicitis update. Curr Opin Pediatr 2011;23(3):281–285.